Journal of Environmental Sciences 161 (2026) 525–535

Contents lists available at ScienceDirect

Journal of Environmental Sciences

journal homepage: www.elsevier.com/locate/jes

JES JOURNAL OF ENVIRONMENTAL SCIENCES www.jesc.ac.cn

Research Article

Photooxidation and ozonolysis of α-pinene and limonene mixtures: Mechanisms of secondary organic aerosol formation and cross-dimerization

Yingqi Zhao[a,b], Ya Zhao[a], Chong Wang[c,d], Yufeng Shao[a,b], Hua Xie[a], Jiayue Yang[a], Weiqing Zhang[a], Guorong Wu[a], Gang Li[a,b,*], Ling Jiang[a,b,e,f,*], Xueming Yang[a,b,c,d,e]

[a] State Key Laboratory of Molecular Reaction Dynamics and Dalian Coherent Light Source, Dalian Institute of Chemical Physics, Chinese Academy of Sciences, Dalian 116023, China
[b] University of Chinese Academy of Sciences, Beijing 100049, China
[c] Institute of Advanced Science Facilities, Shenzhen 518107, China
[d] Department of Chemical Physics, University of Science and Technology of China, Hefei 230026, China
[e] Hefei National Laboratory, Hefei 230088, China
[f] Department of Chemistry and Guangdong Provincial Key Laboratory of Catalytic Chemistry, Southern University of Science and Technology, Shenzhen 518055, China

ARTICLE INFO

Keywords:
Secondary organic aerosol
Monoterpene oxidation
Cross reaction
α-Pinene
Limonene

ABSTRACT

Elucidating the interplay between different volatile organic compounds (VOCs) is crucial for understanding the formation mechanisms of secondary organic aerosols (SOA). This study systematically investigated the interactions between the bicyclic monoterpene α-pinene and the monocyclic monoterpene limonene under NO_2 photooxidation and dark ozonolysis conditions. The results show that under the NO_2 photooxidation conditions, the increase of $[limonene]_0$ enhances particle mass concentrations, number concentrations, and particle size; the increase of $[\alpha\text{-pinene}]_0$ results in the increase of particle mass and number concentrations without the increase of particle size. Under the dark ozonolysis conditions, particle mass and number concentrations increase with the increase of $[\alpha\text{-pinene}]_0$ and $[limonene]_0$; the effect of increasing $[\alpha\text{-pinene}]_0$ on SOA mass concentration is significantly smaller than that of increasing $[limonene]_0$, which may be attributed to the shift to a smaller particle size with the increase of $[\alpha\text{-pinene}]_0$. As the $[limonene]_0/[mixed\ VOCs]_0$ ratio increases from 0 % to 100 %, the SOA yield increases from 54.6 % to 65.2 % under the NO_2 photooxidation conditions and from 19.8 % to 26.2 % under the O_3 conditions. Using threshold photoionization mass spectrometry based on a vacuum ultraviolet free electron laser, a series of new products were detected at molecular weights of 364, 366, 380, 386, 411, 413, and 414, which could be assigned to the cross-dimers, such as organic peroxides, ester dimers, and organic nitrates. Our study underscores the critical role of monocylic monoterpene limonene in the SOA formation and advances our understanding of the SOA formation in the atmosphere.

1. Introduction

Secondary organic aerosols (SOA) are important components of global atmospheric fine particulate matter, which not only play a vital role in atmospheric radiation balance and climate system (Seinfeld et al., 2016; Shrivastava et al., 2017), but also are closely related to respiratory human health problems (Burnett et al., 2018; Jimenez et al., 2009; Lelieveld et al., 2015). Volatile organic compounds (VOCs) undergo oxidation reactions with atmospheric oxidants to generate SOA, which make significant contribution to new particle formation (NPF) (Atkinson, 2000; Atkinson and Arey, 2003) and climate change (Hallquist et al., 2009). With the decrease of atmospheric SO_2 emissions (Daellenbach et al., 2020), the oxidation of biogenic VOCs (BVOCs) to form SOA would become a key driver of NPF, especially in preindustrial regions (Griffin et al., 1999; Kirkby et al., 2016). Monoterpenes are one important class of BVOCs, which are the main global sources of SOA formed from the reactions of BVOCs with ozone (O_3), hydroxyl radicals (OH), and nitrogen oxides (NO_x) in the atmosphere (Guenther et al., 2012; Kelly et al., 2018; Watne et al., 2017; Yao et al., 2022).

As the most abundant monoterpene in the atmosphere, α-pinene has become a focal point of SOA studies (Guenther et al., 1995; Kenseth et al., 2023; Thomsen et al., 2021; Zhang et al., 2019). Unlike α-pinene with a double ring structure, limonene has a single ring structure (Appendix A Fig. S1) and exhibits higher reactivity due to its two double bonds (Appendix A Table S1) (Piletic and Kleindienst, 2022; Saathoff et al., 2009). Even though α-pinene and limonene are isomeric (Appendix A Fig. S1), remarkable differences in the products and yields of SOA have been found during their atmospheric oxida-

* Corresponding authors at: University of Chinese Academy of Sciences, Beijing 100049, China.
E-mail addresses: gli@dicp.ac.cn (G. Li), ljiang@dicp.ac.cn (L. Jiang).

https://doi.org/10.1016/j.jes.2025.04.020
Received 14 January 2025; Received in revised form 4 April 2025; Accepted 9 April 2025
Available online 11 April 2025

tion (Jonsson et al., 2007; Mutzel et al., 2021; Spittler et al., 2006). The volatility of SOA formed from both the photooxidation and dark ozonolysis reactions of α-pinene was slightly higher than that formed from limonene (Kim and Paulson, 2013). As compared to α-pinene, the single-ring structure of limonene facilitates the direct addition of O_2, resulting in a higher yield of oxidation products (Piletic and Kleindienst, 2022). These results provided important insights for understanding the different roles of monocyclic and bicyclic BVOCs in the SOA formation mechanisms and for assessing the complexity of their impacts on atmospheric chemistry and climate.

Recently, increasing efforts have been made to study the roles of VOCs mixtures in the SOA formation mechanisms (Berkemeier et al., 2020; Chen et al., 2022; Dada et al., 2023; Kiendler-Scharr et al., 2009; Li et al., 2007, 2021; McFiggans et al., 2019; Voliotis et al., 2021, 2022; Ylisirnioe et al., 2020; Zhu et al., 2024). Early studies showed that the presence of isoprene significantly suppressed NPF and reduced particle number concentration due to the high reactivity of isoprene toward OH radicals (Kiendler-Scharr et al., 2009). By suppressing the reactions between OH radicals and monoterpenes, isoprene scavenged the highly oxygenated products, which lowers the yield of low-volatility products and consequently suppresses the NPF (McFiggans et al., 2019). Interestingly, the addition of only 2 % sesquiterpenes to the isoprene + α-pinene mixtures remarkably increased the yields of ultralow-volatility organic compounds and doubled the rates of particle formation (Dada et al., 2023). While the oxidation of mixtures of bicyclic monoterpenes (α-pinene) and chain monoterpenes (myrcene) generally leaded to a significant increase of particle mass concentrations (Ahlberg et al., 2017), this phenomenon has not been observed in the two structurally similar mixtures of bicyclic monoterpenes (α-pinene and Δ^3-carene) (Thomsen et al., 2022). When the mixture of α-pinene (the bicyclic monoterpene) and limonene (the monocyclic monoterpene) underwent photooxidation reaction, the SOA yield for α-pinene increased by 50 % but that for limonene decreased by 20 % (Takeuchi et al., 2022). These studies underscored the intricate nonlinear interactions among different types of monoterpenes in the SOA formation, emphasizing the need to incorporate such complexities into atmospheric models. Thus far, systematical studies of the effects of mixing ratios of monocyclic and bicyclic monoterpenes on the SOA formation mechanisms remain scarce.

This study aims to elucidate the interplay between α-pinene (the bicyclic monoterpene) and limonene (the monocyclic monoterpene) for the NO_2 photooxidation and dark ozonolysis reactions. We investigated the effects of the initial concentrations of α-pinene ($[\alpha\text{-pinene}]_0$) and limonene ($[\text{limonene}]_0$) on the mass concentration, number concentration, particle size distribution, and the yield of SOA formed from the BVOCs mixtures. The chemical compositions of SOA were systematically analyzed by using the aerosol mass spectrometry (AMS) based on threshold photoionization with a tunable vacuum ultraviolet free electron laser (VUV-FEL). Combined with quantum chemical calculations, plausible formation mechanisms for the newly observed peroxide and ester cross dimers were proposed. This work highlights the complexity of BVOCs mixture oxidation and underscores the crucial role of monocyclic monoterpenes in the SOA formation of cyclic monoterpene systems.

2. Material and methods

All the experiments were conducted by using the VUV-FEL-based AMS apparatus coupled with a smog chamber. Detailed experimental and calibration procedures can be found in the previous study (Zang et al., 2022) and Appendix A Text S1. A brief overview is provided here. The zero air was supplied by a air compressor, passed through a refrigerated dryer (Model F11, Atlas Copco, Sweden), and further purified using molecular sieves, activated carbon, and a Hopcalite catalyst. The temperature of the smog chamber was maintained at 297 ± 0.5 K and the relative humidity was less than 3 %.

Before the α-pinene + limonene + NO_2 photooxidation and α-pinene + limonene + O_3 dark ozonolysis experiments, the chamber was flushed with purified dried zero air until the concentrations of gaseous substances (e.g., NO_x, O_3, and VOCs) were below their respective detection limits. A known quantity of NO_2 or O_3 was precisely controlled by using calibrated gas cylinders and flow controllers. α-Pinene (99.0 %, Aladdin) and limonene (99.0 %, Aladdin) were introduced into the reactor via the inlet port. To avoid experimental errors caused by changes in the VOCs injection sequence, α-pinene was consistently injected before limonene, as detailed in Appendix A Text S1. O_3 was generated by corona discharge using an ozone generator (Model OZ-3 G, BNP Ozone technology Co., China). All photooxidation and ozonolysis experiments were conducted under seed-free aerosol conditions. For the α-pinene + limonene + NO_2 photooxidation experiments, the reactants (i.e. α-pinene, limonene, and NO_2) were uniformly mixed and the concentration was basically stable for about 30 min, and then the 40 black lamps were turned on for about 300 min. For the α-pinene + limonene + O_3 experiments in the dark, the reactants (i.e., α-pinene, limonene, and O_3) were mixed uniformly for 30 min before turning off the fan. By repeating the 986 ppbV α-pinene + 253 ppbV limonene + 402 ppbV NO_2 experiments, the uncertainty in particle mass concentration was estimated to be < 9.0 % (Appendix A Fig. S2). As detailed in Appendix A Table S2, the uncertainties are shown systematically for all measured instrument parameters.

The components of gas phase and particle phase in the smog chamber were characterized by a series of instruments. NO_x concentrations were monitored by using a gas analyzer (Model 42i, Thermo Fisher Scientific, USA). O_3 concentrations were monitored by using a gas analyzer (Model 49i, Thermo Fisher Scientific, USA). The concentrations of VOCs were monitored by a proton transfer reaction-mass spectrometer (PTR-QMS 3500, East & West Analytical Instruments, China). The concentrations of VOCs were determined by the fragment ion at $m/z = 137$. The particle number concentrations and size distributions were measured by using a Scanning Mobility Particle Sizer (SMPS 3938NL76). The particle mass concentrations were calculated based on the volume concentrations measured by the SMPS, assuming a density of 1.0 g/cm^3 for SOA formed from the oxidation of α-pinene and limonene. Considering SOA generated in the smog chamber could deposit onto the reactor walls (Bian et al., 2015), the wall-loss correction for particles was performed by using the method described by Pathak et al. (2007) with the assumption that the wall loss rate was first order and that the loss rate constant was independent of particle size. The SOA yield was determined as the ratio of the corrected particle mass concentration to the VOCs consumption.

Particles were transmitted through the smog chamber to a Time-of-Flight Mass Spectrometer (TOF-MS) via a silicone tube, a 100 μm diameter critical orifice, and an aerodynamic lens. Then, the particles were deposited onto a copper target in the ionization chamber of TOF-MS and were thermally vaporized by using a heater. Photoionization was carried out with VUV-FEL and the mass spectra of aerosol chemical components were measured in positive ion mode. The tunable VUV-FEL (50-150 nm) enables highly sensitive and selective ionization of SOA, which has been demonstrated applications in probing complex terpene oxidation reactions including isoprene + NO + SO_2 photooxidation (Zhang et al., 2024) and α-pinene + NO_x + NH_3 photooxidation (Zhao et al., 2024). The present TOF-MS mass spectral peaks stand for the molecular weight (MW) values. To minimize the fragmentation, appropriate VUV-FEL wavelengths and pulse energies were optimized to achieve molecular threshold ionization (Zang et al., 2022). The optimal experimental conditions were determined by varying the VUV-FEL wavelength, pulse energy, $[\alpha\text{-pinene}]_0$, $[\text{limonene}]_0$, $[NO_2]_0$, and $[O_3]_0$. Due to the limitation of VUV-FEL beamtime, aerosol mass spectra were representatively measured for a few experimental conditions.

Quantum chemical calculations were performed. The structural optimization and frequency calculations for α-pinene, limonene, their intermediates, transition states, and products involved in the whole pathways

Table 1 – Overview of the α-pinene and limonene photooxidation experimental conditions.

$[\alpha\text{-Pinene}]_0$ (ppbV)	$[\text{Limonene}]_0$ (ppbV)	$[NO_2]_0$ (ppbV)	ΔM ($\mu g/m^3$)	ΔROG (ppbV)	SOA yields (%)
994	0	404	3005	989	54.6
986	253	402	3401	1134	55.9
979	481	396	4530	1446	56.3
995	967	408	5936	1804	59.2
954	990	396	5808	1798	58.1
484	978	415	4780	1422	60.4
244	970	418	3555	1018	62.8
0	987	392	3433	947	65.2

$[X]_0$: the initial concentration of the species X; ΔM: the mass concentration of formed SOA; ΔROG: the amount of reacted organic gases; SOA: secondary organic aerosol.

Table 2 – Overview of the α-pinene and limonene ozonolysis experimental conditions.

$[\alpha\text{-Pinene}]_0$ (ppbV)	$[\text{Limonene}]_0$ (ppbV)	$[O_3]_0$ (ppbV)	ΔM ($\mu g/m^3$)	ΔROG (ppbV)	SOA yields (%)
976	0	242	760	690	19.8
989	246	240	1073	850	22.7
994	512	245	1310	1017	23.1
991	980	243	1469	1138	23.2
975	971	253	1514	1146	23.7
564	977	244	1372	1022	24.1
236	968	250	1157	845	24.6
0	978	243	1074	738	26.2

were carried out by using the Gaussian 16 software (Frisch et al., 2016) at the M06–2X/def2-TZVP level of theory. Single-point energy calculations were conducted with the ωB97XD/aug-cc-pVTZ method. The selection of such theoretical method was based on our recent studies on the effects of isoprene on the ozonolysis of Δ^3-carene and β-caryophyllene (Zhang et al., 2025). The detailed theoretical methods are provided in Appendix A Text S1.

3. Results and discussion

The experimental conditions for NO_2 photooxidation of α-pinene and limonene are shown in Table 1 and those for O_3 dark reactions of α-pinene and limonene in Table 2, respectively. By setting different initial concentration combinations of α-pinene and limonene, the interactions between α-pinene and limonene were investigated in depth to evaluate their impacts on the particle mass concentrations, number concentrations, and size distributions. Further analysis of the impact of different initial limonene ratios on SOA yield aims to clarify how $[\text{limonene}]_0/[\text{mixed VOCs}]_0$ influenced the formation of SOA. Based on the VUV-FEL aerosol mass spectra and quantum chemical calculations, the structural characteristics of cross-dimers formed through VOC-cross reactions were analyzed in detail.

3.1. Effects of $[\alpha\text{-pinene}]_0$ and $[\text{limonene}]_0$ on particle mass concentrations, number concentrations, and size distributions

The temporal evolution of particle mass concentrations (Fig. 1a and b) and particle size distributions (Fig. 1c and d) for the NO_2 photooxidation reactions under various initial concentration combinations of α-pinene and limonene is illustrated in Fig. 1. The maximum particle mass concentration and peak value of particle size in the 994 ppbV α-pinene + 404 ppbV NO_2 condition is 3005 $\mu g/m^3$ and 71 nm (Fig. 1a and c, black curve), respectively, and that in the 987 ppbV α-pinene + 392 ppbV NO_2 condition is 3433 $\mu g/m^3$ and 126 nm (Fig. 1b and d, black curve). This indicates that the NO_2 photooxidation of limonene produces slightly higher particle mass concentration and significantly larger particle size than that of α-pinene. As compared to the α-pinene-OH adducts, the limonene-OH adducts do not require extra energy to break a ring during the initial oxidation step (Piletic and Kleindienst, 2022), facilitating the condensation of low-volatility oxidation products and resulting in a higher particle mass concentration and a larger particle diameter (Hanson et al., 2022; Liu et al., 2023; Zhao et al., 2018). Previous studies indicated that the concentration of carboxylic acids produced from α-pinene ozonolysis is higher that from Δ^3-carene within 15 min, which aligns with the evolution of particle mass concentrations (Thomsen et al., 2022). Accordingly, the more pronounced impact of limonene on particle mass concentrations and size distributions might be primarily attributed to the higher reactivity of limonene and the contribution of different oxidation products.

In the photooxidation experiments of ~990 ppbV α-pinene + x ppbV limonene + ~400 ppbV NO_2 mixed VOCs, an increase of $[\text{limonene}]_0$ leads to a significant increase of particle mass concentration (Fig. 1a), accompanied by an increase of particle number concentration (Appendix A Fig. S3) and particle size (Fig. 1c). This indicates that higher $[\text{limonene}]_0$ in the α-pinene + limonene + NO_2 mixtures helps to produce more low-volatility compounds, promoting particle growth and condensation. In the photooxidation experiments of x ppbV α-pinene + ~980 ppbV limonene + ~400 ppbV NO_2 mixed VOCs, when the $[\alpha\text{-pinene}]_0$ is increased, both particle mass concentration and number concentration (Fig. 1b and d, and Appendix A Fig. S3) show a remarkable rise, whereas the particle size distribution moves to a smaller size. It has been demonstrated that the concentrations of RO_2 radicals and closed-shell extremely low volatility organic compounds (ELVOCs) generated from α-pinene are lower than those from limonene (Jokinen et al., 2015). Given that ELVOCs undergo irreversible condensation onto surfaces, they are expected to significantly contribute to the growth of newly formed particles (Ehn et al., 2014). Then, the shift in particle size distribution to smaller size when increasing $[\alpha\text{-pinene}]_0$ may be due to the lower concentrations of RO_2 radicals and closed-shell ELVOCs, as well as the molecular composition, volatility and the ratio of oligomeric compounds (Liu et al., 2024). These findings suggest that limonene plays a more pronounced role in the promotion of particle growth in mixed monoterpene photooxidation reactions. In contrast with aforementioned pure NO_2 photooxidation experiments, the 97 ppbV α-pinene + 42 ppbV limonene + 106 ppbV NO + 41 ppbV NO_2 reaction showed a time delay of approximately 3 h because of the transform from NO to NO_2 (Li et al., 2007).

The importance of monoterpene ozonolysis in the formation of SOA in the atmosphere has been widely recognized (Griffin et al., 1999; Saathoff et al., 2009; Ye et al., 2018). For the photooxidation of monoterpenes, the photolysis of NO_x generates O_3, which triggers the oxidation of monoterpenes (Luo et al., 2021; Wildt et al., 2014). The temporal evo-

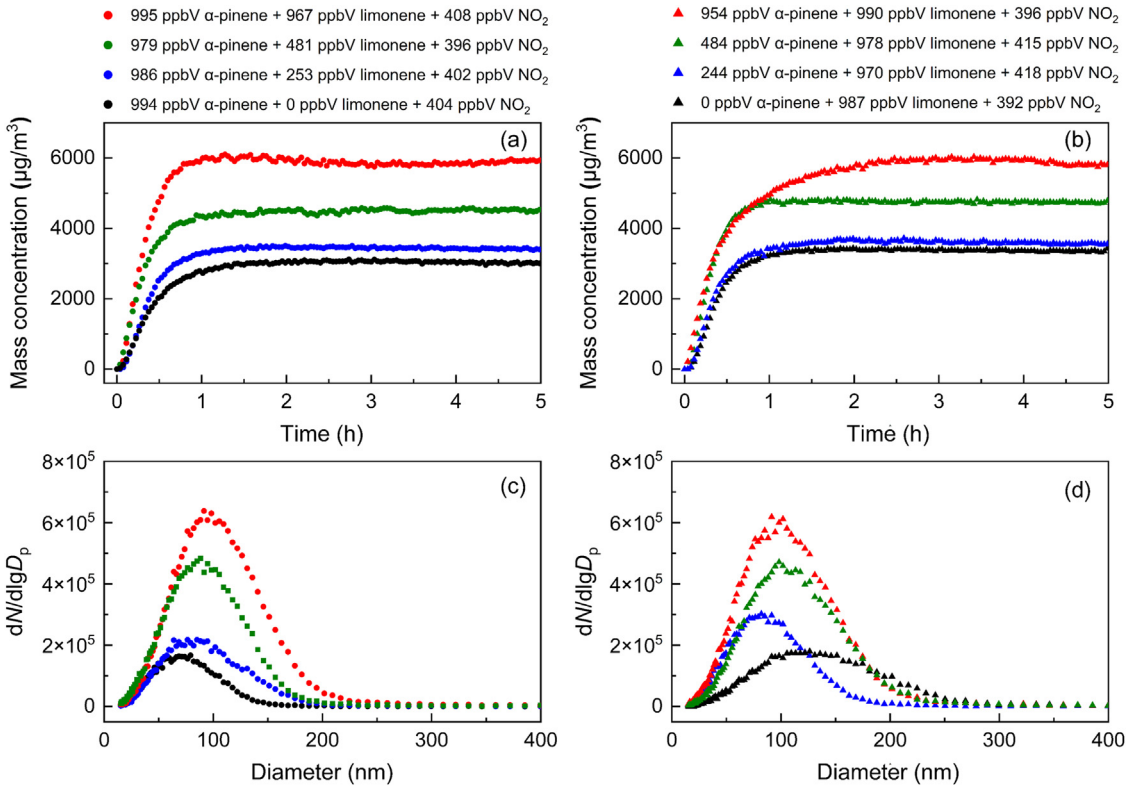

Fig. 1 – Particle mass concentrations (a and b) and size distributions (c and d) as a function of the initial concentration of α-pinene and limonene for the α-pinene + limonene + NO_2 reactions. D_p: particle diameter; $dN/dlgD_p$: normalized number size distribution.

lution of particle mass concentration and size distribution for the dark reactions of α-pinene and limonene with O_3 is illustrated in Fig. 2. The maximum particle mass concentration and peak value of particle size in the 976 ppbV α-pinene + 242 ppbV O_3 condition is 760 $\mu g/m^3$ and 102 nm (Fig. 2a and c, black curve), respectively, and that in the 978 ppbV limonene + 243 ppbV O_3 condition is 1074 $\mu g/m^3$ and 109 nm (Fig. 2b and d, black curve). These results show that the ozonolysis of limonene forms particles with higher mass concentration and slightly larger particle size than that of α-pinene, which holds true for particle number concentration (Appendix A Fig. S4). The SOA yields generated from the ozonolysis of α-pinene and limonene were found to be higher than those from the OH radical oxidation (Zhao et al., 2015). Additionally, the volatility of SOA formed from the ozonolysis of monoterpenes (α-pinene, β-pinene and limonene) is lower than those from the OH radical oxidation (Watne et al., 2017). Accordingly, the SOA components could be dominated by O_3 oxidation rather than OH radical oxidation. Then, the higher particle mass/number concentration and larger particle size of limonene than that of α-pinene could be due to the high reaction rate (Appendix A Table S1) and lower barrier (Appendix A Fig. S5) of the reaction between limonene and O_3 as compared to the reaction between α-pinene and O_3, which leads to a higher relative abundance of highly oxygenated organic molecules (HOMs) and low-volatility compounds in the ozonolysis products of limonene (Jonsson et al., 2007; Kim and Paulson, 2013; Liu et al., 2023).

In the ozonolysis reactions of ~990 ppbV α-pinene + x ppbV limonene + ~240 ppbV O_3 mixed VOCs, the increase of $[\text{limonene}]_0$ results in a significant rise in particle mass concentration (Fig. 2a) and number concentration (Appendix A Fig. S4b_1-d_1), while the particle size distribution shows no substantial change in diameter (Fig. 2c). In the ozonolysis reactions of x ppbV α-pinene + ~980 ppbV limonene + ~240 ppbV O_3 mixed VOCs systems, when the $[\alpha\text{-pinene}]_0$ is increased, particle mass concentration and number concentration slightly increase (Fig. 2b and Appendix A Fig. S4), whereas particle size slightly decreases (Fig. 2d). These findings suggest that the increase of $[\alpha\text{-pinene}]_0$ in the mixed VOCs system shows a smaller enhancement of particle mass concentration and number concentration than the increase of $[\text{limonene}]_0$. This difference highlights the higher reactivity of limonene with O_3, which produces a larger quantity of low-volatility oxidation products and consequently promotes the SOA formation.

Under both α-pinene + limonene + NO_2 photooxidation and α-pinene + limonene + O_3 dark conditions, limonene exhibits a more pronounced promotion effect on particle mass concentrations than α-pinene (Figs. 1 and 2), implying that limonene exhibits higher reactivity for both photooxidation and dark ozonolysis reaction, and limonene oxidation products have a more significant contribution to particle mass concentrations and size distributions. We found in the photooxidation and dark ozonolysis of α-pinene and limonene mixed systems, the presence of α-pinene shifts the particle size distribution toward smaller sizes. Recent studies have demonstrated that the particle mass concentration formed from the ozonolysis of a mixture of the bicyclic terpenes of α-pinene and Δ^3-carene is comparable to that from α-pinene alone (Thomsen et al., 2022). Our findings are consistent with recent studies that the monocyclic monoterpene of limonene plays an important role in the formation of SOA due to its high reactivity toward ozonolysis in the mixed cyclic monoterpenes (Takeuchi et al., 2022). The presence of acyclic monoterpenes in the mixture of monoterpene was also found to facilitate the formation of larger particle diameters (Ahlberg et al., 2017). Given the high proportion of cyclic monoterpenes in the real atmosphere, the monocyclic monoterpene limonene could contribute more significantly to the particle mass concentration and size distribution within mixtures of monocyclic and bicyclic monoterpene.

The concentration variations and the reactivity of monoterpenes are critical factors for the influence of SOA formation in multi-VOC precursor systems (Takeuchi et al., 2022). Notably, the number of double bonds in the monoterpenes directly affects the yields of SOA (Hanson et al., 2022). The interactions among different VOCs and their

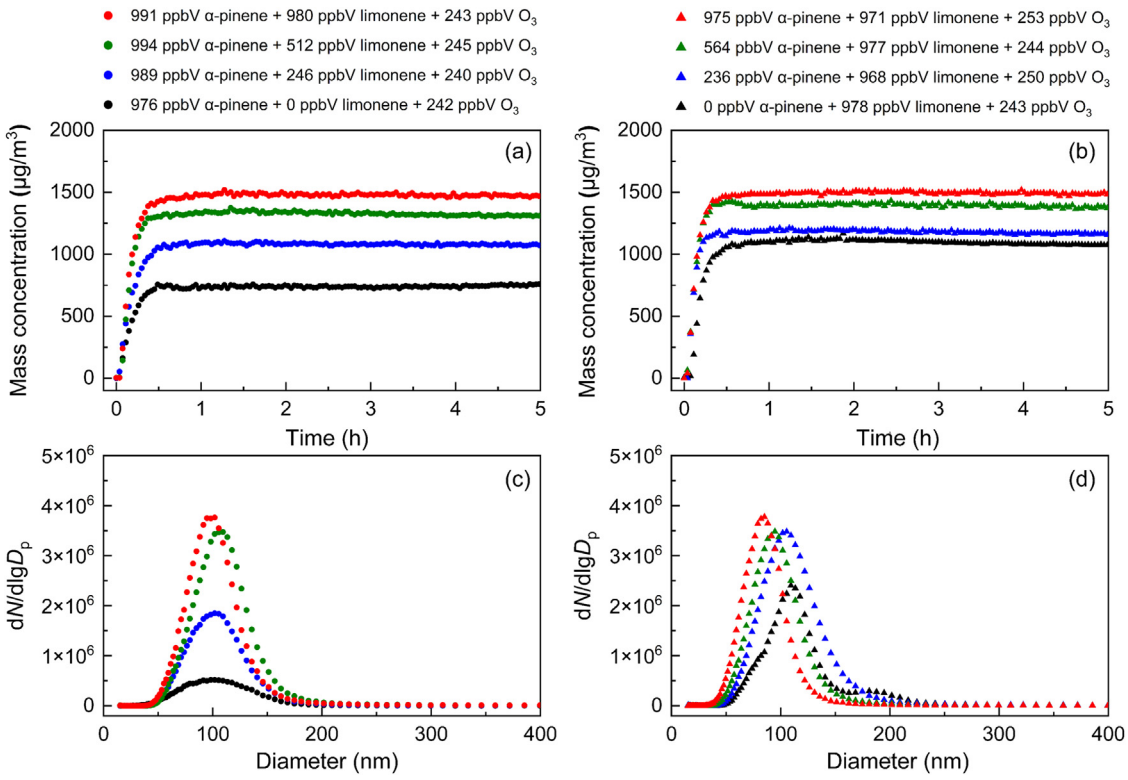

Fig. 2 – Particle mass concentrations (a and b) and size distributions (c and d) as a function of the initial concentration of α-pinene and limonene for the α-pinene + limonene + O_3 reactions.

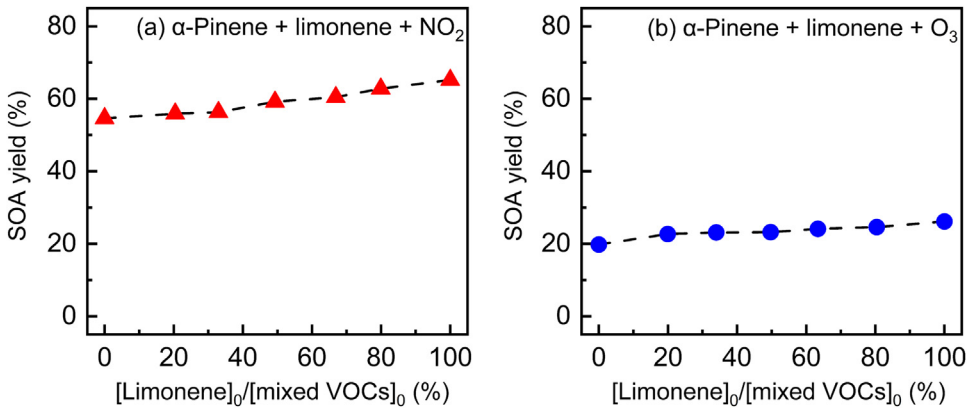

Fig. 3 – SOA yields as a function of $[limonene]_0/[mixed\ VOCs]_0$. The red triangle and blue dot icons represent the reaction of α-pinene + limonene + NO_2 (a) and α-pinene + limonene + O_3 (b), respectively. SOA: secondary organic aerosol.

complex reaction pathways can lead to variations in the chemical compositions, volatility of aerosols, and the yields of SOA (Liu et al., 2024). Previous studies have demonstrated that, within mixed VOCs systems, the influence of the proportion of limonene is significantly greater than that of VOC/NO_x ratios, ambient temperature, and light intensity (Li et al., 2007). As shown in Fig. 3, with the increase of the $[limonene]_0/[mixed\ VOCs]_0$ ratio from 0 to 100 %, the SOA yield increases from 54.6 % to 65.2 % under NO_2-induced photooxidation conditions (Fig. 3a) and increases from 19.8 % to 26.2 % under ozonolysis conditions (Fig. 3b). This trend suggests that a larger proportion of limonene in the mixed VOCs systems helps to improve the SOA yields under both NO_2 photooxidation and dark ozonolysis conditions. Our results are consistent with previous studies that the addition of a small amount of limonene increased the SOA yield in the α-pinene system by 50 % (Takeuchi et al., 2022). The time evolutions of O_3 concentration during the NO_2 photooxidation and O_3 dark reactions under different experimental conditions are shown in Appendix A Figs. S6 and S7, respectively. As exemplified in a comparison between two experimental conditions 986 ppbV α-pinene + 253 ppbV limonene + 402 ppbV NO_2 (Appendix A Fig. S6b_1) and 989 ppbV α-pinene + 246 ppbV limonene + 240 ppbV O_3 (Appendix A Fig. S6b_2), the time-weighted average O_3 concentration over the 5 h photooxidation period (90 ppbV) is significantly higher than that under dark reaction condition (16 ppbV). While NO_3 radical is known to contribute to SOA formation, particularly under nighttime conditions, the impact of NO_3 radical during α-pinene and limonene photooxidation is minimal because of their rapid photolysis under illuminated conditions. The higher SOA yields observed in the NO_2 photooxidation system (Fig. 3a) than those in dark ozonolysis conditions (Fig. 3b) are more likely driven by the higher average O_3 concentration from NO_2 photolysis and OH radical production (Draper et al., 2015; Luo et al., 2023), the influence of NO_3 radicals plays only a minor role.

3.2. VUV-FEL photoionization mass spectra of photooxidation of α-pinene and limonene

In this study, the mass spectra of particle components were continuously monitored after the particles appeared. As the particle mass concentration increases, the intensities of the mass spectra gradually increase. Taking the photooxidation of 995 ppbV α-pinene + 967 ppbV limonene + 408 ppbV NO_2 as an example, the time distribution of the monomer intensities is shown in Appendix A Fig. S8. During the continuous detection, the positions of mass spectral peaks do not show significant changes. The mass spectra corresponding to the time of maximum particle mass concentration were selected for analysis. The results under different experimental conditions are systematically compared to explore the formation of monomer and dimer products and the possible reaction pathways.

The photoionization mass spectra of the products formed from NO_2 photooxidation and dark ozonolysis reactions of α-pinene and limonene are presented in Appendix A Fig. S9. All numerical markers in Appendix A Fig. S9 represent the MW of compounds and the molecular formula of compounds are listed in the Appendix A Table S3. As shown in Appendix A Fig. S9a_1 and c_1, under NO_2 photooxidation conditions, the monomer products (120 < MW < 220) of limonene exhibit stronger signal intensities than those of α-pinene. These results of mass spectra suggest that under identical photooxidation conditions, limonene is more likely to form monomer products. Under ozonolysis conditions (Appendix A Fig. S9a_2 and c_2), the signal intensities of MW = 200 ($C_{10}H_{16}O_4$) and MW = 216 ($C_9H_{12}O_6$) for limonene are much higher than those for α-pinene. However, the intensity of MW = 184 ($C_{10}H_{16}O_3$) for limonene is weaker than that for α-pinene (Appendix A Fig. S9a_2 and c_2). This indicates that the monomer products formed from limonene have a higher oxygen content than those formed from α-pinene.

In contrast with the single VOC system (Appendix A Fig. S9$a_{1,2}$ and $c_{1,2}$), mass spectra of the mixed VOCs system (Appendix A Fig. S9b_1 and b_2) reveal a significant enhancement in the intensities of the monomer signals (120 < MW < 220). This may be rationalized that the oxidation of both α-pinene and limonene could form the monomer products with identical molecular weights but with different structures. The signals of the dimer products (MW = 350-420) for the mixed VOCs system are much more than those for the single VOC system, especially at MW = 364, 366, 380, 386, 411, 413, and 414, implying that the cross reactions might occur in the oxidation of the mixed VOCs system. In contrast with the α-pinene + limonene + O_3 dark condition (Appendix A Fig. S9b_2), the products of MW = 411 and 413 were observed in the α-pinene + limonene + NO_2 photooxidation reaction (Appendix A Fig. S9b_1), which may be attributed to the nitrogen-containing dimers. In the atmosphere, the cross-reactions of RO_2 radicals exhibit a high reaction rate, leading to the formation of accretion products through the reaction $RO_2 + R'O_2 \rightarrow ROOR' + O_2$ (Berndt, et al., 2018a). Recently, a nucleophilic addition mechanism of particle-phase alcohols and cyclic acylperoxyhemiacetals has been proposed (Kenseth et al., 2023). In this study, the cross-reactions in the oxidation of α-pinene and limonene could be driven by the interactions between their primary oxidation products (vide infra), including the cross-reaction of RO_2 radicals to form more complex dimers and the nucleophilic addition between C9 and C10 monomers to form thermally stable accretion products (Kenseth et al., 2023; Takeuchi et al., 2022).

3.3. Analysis of chemical compositions and formation mechanisms of products

To understand the structures and possible formation mechanisms of the products formed from photooxidation and ozonolysis of α-pinene and limonene, we performed quantum chemical calculations. For the NO_2 photooxidation of α-pinene and limonene, O_3 generated from NO_2 photolysis serves as the main oxidant. For the ozonolysis of α-pinene and limonene, O_3 also triggers the primary oxidation. Accordingly, the possible reaction pathways of α-pinene and limonene with O_3 are shown in Appendix A Fig. S10, highlighting the key steps involved in the formation of major intermediates and products, including O_3 addition to double bond, O_2 addition, intramolecular hydrogen-shift (H-shift), and decomposition reactions. For the reaction of α-pinene and O_3, O_3 undergoes an addition reaction with the molecular double bond to form the primary ozonide (POZ), which subsequently undergoes the decomposition reaction to generate intermediate A1, which is calculated to be highly exothermic by 77.3 kcal/mol with an O_3 addition barrier of 3.1 kcal/mol and a POZ decomposition barrier of 22.3 kcal/mol, respectively. The A1 → A2 reaction is exothermic by 23.6 kcal/mol with an intramolecular H-shift barrier of 12.7 kcal/mol, which aligns with the previously reported molecular mechanism for rapid autoxidation in the α-pinene ozonolysis (Iyer et al., 2021). The reaction of A2 → P-A-1 (MW = 184) and A2 → P-A-2 (MW = 200) is exothermic of 11.2 kcal/mol and 85.3 kcal/mol, respectively, which two products have been reported recently (Iyer et al., 2021; Jia and Xu, 2020; Zhao et al., 2024). Notably, the α-pinene-formed A2 and the limonene-formed L5 undergo a cross-reaction with the loss of HCHO and O_2 to form A3, which is highly exothermic by 100.3 kcal/mol. Following the ozonolysis of the double bond in A3, VOC-cross reaction product CP-1 (MW = 386) is formed, which is predicted to be extremely exothermic by 180.3 kcal/mol with the O_3 addition barrier of 5.1 kcal/mol and the POZ decomposition barrier of 23.4 kcal/mol (loss of HCOOH).

For the oxidation of limonene, the limonene → L2 reaction is predicted to be exothermic (96.7 kcal/mol) with a smaller O_3 addition barrier (1.1 kcal/mol) and a smaller decomposition barrier (20.6 kcal/mol) than the α-pinene → A2 reaction. L2 further reacts with NO to form L3, which is exothermic by 12.3 kcal/mol. L3 undergoes the H-shift reaction and reacts with O_2 to produce L4, which is exothermic by 53.9 kcal/mol with the H-shift reaction barrier of 8.9 kcal/mol. The L4 → P-L-1 (MW = 214) is calculated to be exothermic (7.9 kcal/mol) with the H-shift barrier of 18.8 kcal/mol. Similar to the L3 → L4 reaction, the autoxidation reaction from L4 to L5 is thermodynamically and dynamically feasible. The limonene-formed L5 and the α-pinene-formed A2 undergo VOC-cross reaction to form CP-2 (MW = 414) through the $RO_2 + R'O_2 \rightarrow ROOR' + O_2$ mechanism, which is predicted to be highly exothermic (38.7 kcal/mol). These results suggest that the VOC-cross products CP-1 and CP-2 may be formed through VOC-cross dimerization between RO_2 radicals generated by ozonolysis of α-pinene and limonene, respectively.

In addition to the cross-reactions between RO_2 radicals (Berndt, et al., 2018b; Perakyla et al., 2023), recent studies suggested that the nucleophilic addition of alcohols to cyclic acylperoxyhemiacetals may also form VOC-cross dimers in the particle phase (Kenseth et al., 2023). The potential formation mechanisms of the products MW = 364, 366, and 380 are shown in Fig. 4. These products may be formed through the VOC-cross-reaction between α-pinene-formed monomer P-A-1 and limonene-formed monomers P-L-*n* (*n* = 1-3), which involve a series of isomerization, nucleophilic addition, and dehydration reactions. During the oxidation of α-pinene and limonene mixture, P-L-1 undergoes ozonolysis and releases HCOOH to form the C9 monomer product P-L-3 (MW = 216), which is highly exothermic (181.7 kcal/mol) with the O_3 addition barrier of 4.2 kcal/mol and the decomposition barrier of 24.9 kcal/mol. Additionally, P-L-1 may also undergo intramolecular isomerization to form the monomer P-L-2 (MW = 214), which is exothermic by 3.2 kcal/mol.

The limonene-formed monomers P-L-1, P-L-2, and P-L-3 could react with α-pinene-formed P-A-1 to form cross-reaction dimers, which processes are analyzed in detail as follows. P-L-1 undergoes nucleophilic addition with P-A-1 to form the acylperoxyhemiacetal L-5, which is exothermic by 10.5 kcal/mol. Based on previously proposed mechanisms (Kenseth et al., 2023), L-5 further reacts with P-A-1, releasing P-A-2 and H_2O and producing CP-3 (MW = 364), which process is exothermic by 76.8 kcal/mol. Similar to the P-L-1 → CP-3 reaction, the P-L-

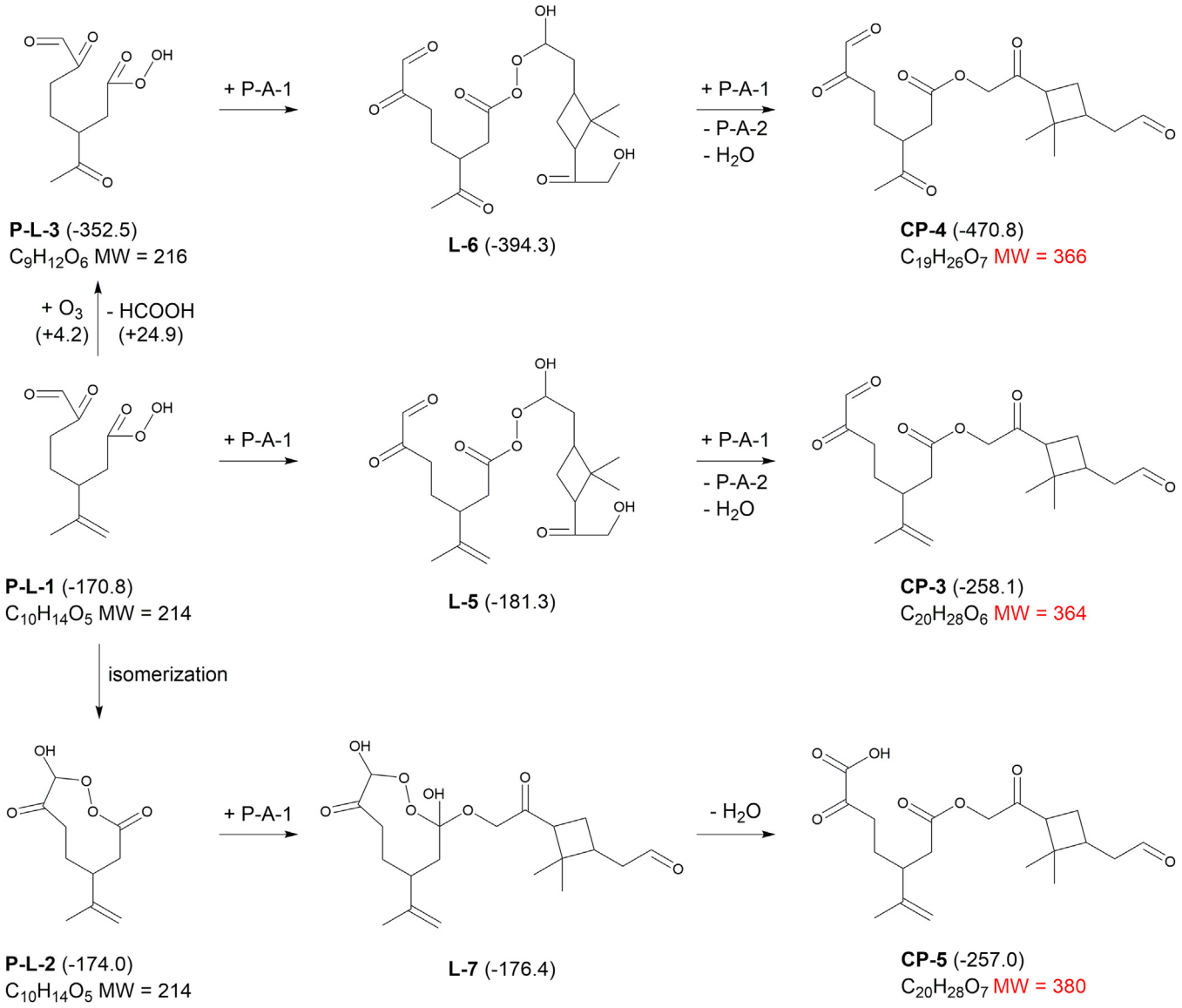

Fig. 4 – Possible formation mechanisms of possible VOC-cross products MW = 364, 366, and 380 calculated at the ωB97XD/aug-cc-pVTZ//M06–2X/def2-TZVP level of theory. Relative energies are given in kcal/mol. MW: molecular weight.

3 → CP-4 (MW = 366) reaction is exothermic by 118.3 kcal/mol. P-L-2 might also participate in the reaction with P-A-1 to form L-7 (MW = 214) with the predicted exothermicity of 2.4 kcal/mol. Then, L-7 loses H_2O to produce CP-5 (MW = 380), which is exothermic by 80.6 kcal/mol. For the photooxidation and ozonolysis of α-pinene and limonene, ester dimer products CP-3, CP-4, and CP-5 are formed through nucleophilic addition of alcohols to acylperoxyhemiacetals and dehydration reactions. As described in Appendix A Fig. S11, the limonene-formed C9 monomer P-L-3 reacts with the α-pinene-formed C10 monomer P-A-1 to generate the C19 dimer CP-4. The C10 monomers P-L-1 and P-L-2 from limonene oxidation and C10 monomer P-A-1 from α-pinene oxidation undergo VOC-cross reactions to form the C20 cross-dimers CP-3 and CP-5.

The potential formation pathways of nitrate ester VOC-cross dimers CP-6 (MW = 411) and CP-7 (MW = 413) formed through nucleophilic addition of alcohols to a cyclic acylperoxyhemiacetal are illustrated in Fig. 5. OH radical plays a key role in the monoterpene photooxidation, promoting the formation of low volatile products (Rolletter et al., 2019). α-Pinene reacts with OH radical to form A5 with the predicted exothermicity of 34.6 kcal/mol. A5 reacts with O_2 to form A6, which is predicted to be highly exothermic by 27.8 kcal/mol. Previous studies indicated that organic nitrates could be generated from the NO_2 photooxidation of α-pinene (Park et al., 2017; Zhao et al., 2018). A6 reacts with NO generated from the photolysis of NO_2 to form the organic nitrate ester P-A-3 (MW = 215), which is predicted to be highly exothermic by 50.3 kcal/mol. The α-pinene-formed P-A-3 reacts with the limonene-formed P-L-2 to form A7, which is exothermic by 9.5 kcal/mol. A7 subsequently loses H_2O to form the organic nitrate cross-product dimer CP-6 (MW = 411) with the predicted exothermicity of 73.0 kcal/mol. The double bond in CP-6 undergoes ozonolysis reaction to form A8, which is a highly exothermic reaction (64.1 kcal/mol) with a very small O_3 addition barrier of 0.4 kcal/mol. A8 loses HCOOH to form CP-7 (MW = 413), which is highly exothermic by 117.5 kcal/mol with the decomposition barrier of 25.0 kcal/mol. Our calculations reveal that in the α-pinene + limonene + NO_2 photooxidation reaction, the monomer P-L-2 derived from limonene oxidation reacts with the organic nitrates P-A-3 derived from α-pinene oxidation to form the cross-dimers CP-6 and CP-7. The results in Figs. 4 and 5 further demonstrate that the limonene-formed monomers (P-L-1, P-L-2, and P-L-3) and the α-pinene-formed monomers (P-A-1 and P-A-3) could undergo nucleophilic addition reac-

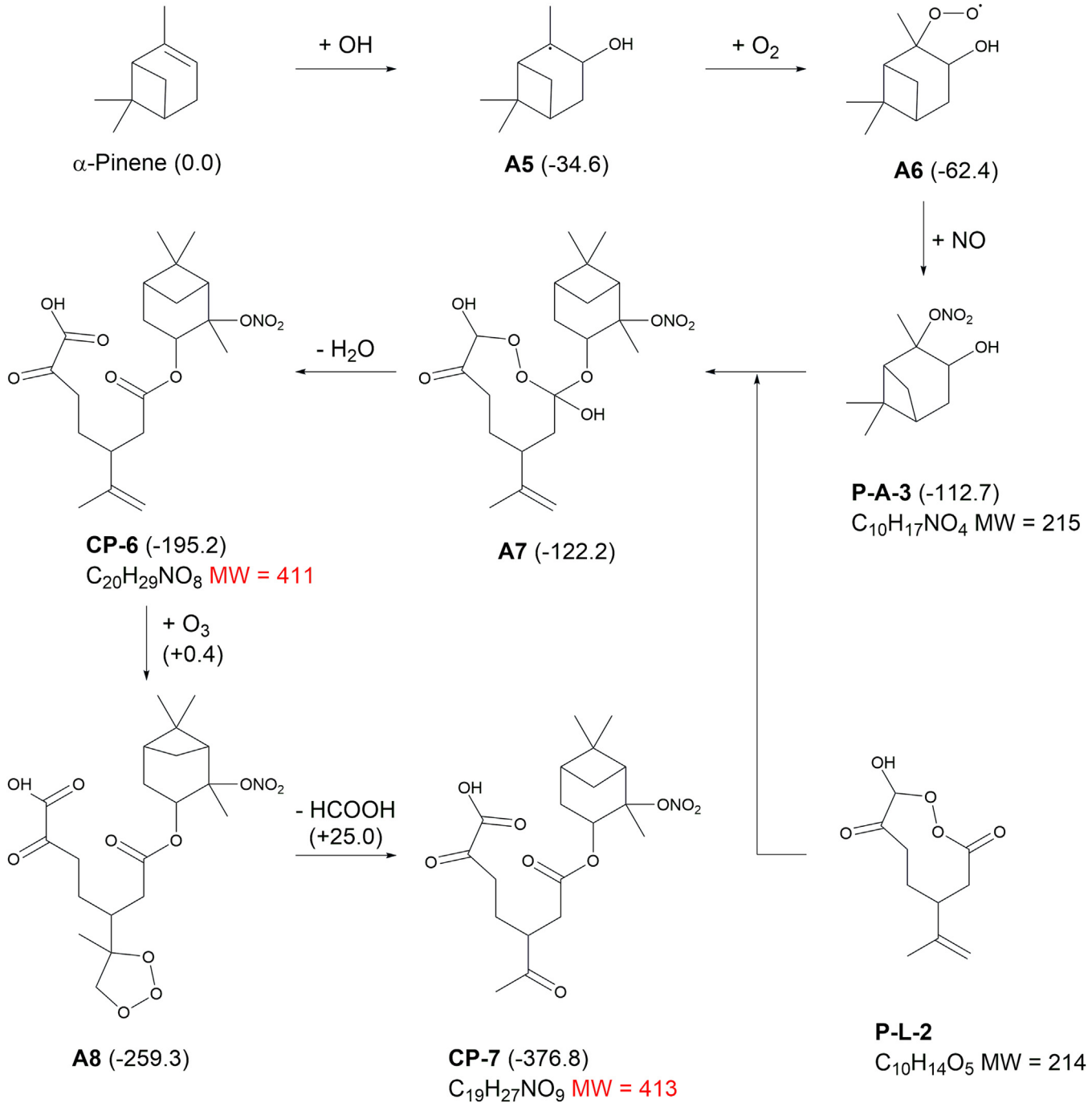

Fig. 5 – Possible formation mechanisms of possible VOC-cross products MW = 411 and 413 calculated at the ωB97XD/aug-cc-pVTZ//M06–2X/def2-TZVP level of theory. Relative energies are given in kcal/mol.

tions of alcohols to acylperoxyhemiacetals, resulting in the formation of the VOC-cross dimers CP-*n* (*n* = 3-7).

4. Conclusions and implication

Gaining a deep understanding of the mechanisms of chemical interactions of oxidation products in the multi-VOC systems is crucial for accurately modelling the SOA formation. In this study, we explored the complex interactions between the bicyclic monoterpene α-pinene and the monocyclic monoterpene limonene during NO_2 photooxidation and dark ozonolysis reaction, with the emphasis on the significant role of $[\alpha\text{-pinene}]_0$ and $[\text{limonene}]_0$ in the influencing of SOA formation. The results demonstrate that under the α-pinene + limonene + NO_2 photooxidation conditions, an increase of $[\text{limonene}]_0$ leads to the enhanced particle mass and number concentrations and a shift in particle size distributions toward larger sizes. In contrast, an increase of $[\alpha\text{-pinene}]_0$ results in higher particle mass and number concentrations but no shift toward larger particle sizes. Under the α-pinene + limonene + O_3 dark conditions, the particle mass and number concentrations show an increase trend with the increase of $[\alpha\text{-pinene}]_0$ and $[\text{limonene}]_0$; the effect of increasing $[\alpha\text{-pinene}]_0$ on SOA mass concentration is significantly smaller than that of increasing $[\text{limonene}]_0$, which may be attributed to a shift to smaller size in particle size distributions with the increase of $[\alpha\text{-pinene}]_0$. As the increase of $[\text{limonene}]_0/[\text{mixed VOCs}]_0$ ratio from

0 to 100 %, the SOA yield increases from 54.6 % to 65.2 % under the α-pinene + limonene + NO_2 photooxidation conditions and increases from 19.8 % to 26.2 % under the α-pinene + limonene + O_3 conditions. In the mixed VOCs system, the proportion of initial limonene concentration plays a more dominant role in the enhancement of SOA yield. Based on the VUV-FEL photoionization mass spectra and quantum chemical calculations, we proposed that the cross-reactions between RO_2 radicals formed from the oxidation of α-pinene and limonene, as well as cross-dimerization driven from nucleophilic addition involving alcohols and acylperoxyhemiacetals, are key mechanisms for the formation of cross-dimers. The RO_2 cross-reactions produce cross-dimers such as CP-1 (MW = 386) and CP-2 (MW = 414), whereas the ester dimer products CP-3 (MW = 364), CP-4 (MW = 366), and CP-5 (MW = 380) are formed through nucleophilic addition reactions of between monomer products. CP-6 (MW = 411) and CP-7 (MW = 413) are identified as nitrogen-containing dimer products.

In recent decades, the length and frequency of the dry seasons in the southern Amazon have increased due to deforestation and climate change (Fu et al., 2013). Additionally, the average temperature in the Amazon region from 1973 to 2013 was observed to be 26.5 °C (Almeida et al., 2017). Our simplified conditions are close to the Amazon dry seasons. Our observations of dimeric species ($C_{18}H_{26}O_9$, $C_{20}H_{30}O_9$, $C_{20}H_{28}O_6$, $C_{19}H_{26}O_7$ and $C_{20}H_{28}O_7$) are consistent with dimeric monoterpene oxidation products ($C_{16–20}H_yO_{6–9}$) observed in the boreal forest in Finland in spring 2013 and 2014 (Mohr et al., 2017). Our present studies could contribute to understand the formation mechanisms of ($C_{16–20}H_yO_{6–9}$) observed in the boreal forest in Finland. Considering the inconclusive formation pathways of these dimers observed by chemical ionization mass spectrometer in the Finnish boreal forest, we hypothesize that the dimeric species in this region may potentially originate from cross-reactions between RO_2 radicals as well as cross-dimerization driven by nucleophilic addition involving alcohols and acylperoxyhemiacetals.

With the increase of RH (20 %-60 %), the yield of limonene-derived SOA increases (Zhang et al., 2023), whereas that of α-pinene-SOA exhibits a minor increase (Jonsson et al., 2006). During the ozonolysis of limonene, the stabilized Criegee intermediate can react with H_2O to form keto-limonene (Zhang et al., 2023). Moreover, SOA yield from the limonene + NO_3 reaction remains relatively stable (~174 %) at 25°C, but varies between 81 % and 148 % at 40 °C (Boyd et al., 2017). SO_2 has been shown to influence SOA formation through multiple pathways, including acid-catalyzed reactions, which create acidic aerosol surfaces that facilitate heterogeneous reactions and oligomerization (Jang et al., 2004). Additionally, SO_2 can interact with Criegee intermediates to form H_2SO_4, which enhances the maximum number concentration of particles and affects both SOA yields and the formation of HOMs (Yang et al., 2023). In real atmospheric conditions, the presence of other VOCs, such as isoprene and o-cresol, can further influence SOA formation. Isoprene competes with monoterpenes for the scavenging of both OH and low-volatility products (McFiggans et al., 2019), but no significant suppression or promotion of particle yield was observed in the mixed system of o-cresol and isoprene (Voliotis et al., 2022). The influence of water vapor, temperature, sulfur dioxide, and other VOCs on the reaction mechanisms and SOA formation will be studied in the future experiments.

The cross-dimerization reactions between gas-phase RO_2 radicals derived from α-pinene and limonene, and oligomerization of their respective oxidation products, have been demonstrated to effectively generate thermally stable C20 and C30 accretion products (Takeuchi et al., 2022). For the limonene + myrcene + OH reactions, the suppression effect on certain C19 dimers in the mixed SOA was also observed compared to β-myrcene SOA, indicative of the presence of complex interactions during the oxidation process of monoterpene mixtures (Liu et al., 2024). Due to the thermal desorption technique employed by a filter inlet for gases and aerosols coupled to a chemical ionization mass spectrometer (FIGAERO-CIMS), thermally unstable oligomers in the experiments may have decomposed. VUV-FEL-based AMS was utilized for online measurements of monoterpene cross-products that are difficult to detect using FIGAERO-CIMS. Based on our proposed mechanism of RO_2 radicals cross-reactions and nucleophilic addition of alcohols to peroxyhemiacetals, we demonstrate that limonene-derived RO_2 radicals and limonene-formed oxidation products (P-L-1, P-L-2, P-L-3) can provide additional binding sites leading to the formation of C18, C19 and C20 VOC-cross dimers to enhance the SOA yield. Our findings emphasize the need for further studies on mixtures of monocyclic terpenes to achieve a more comprehensive understanding of the complex chemical reaction networks that emerge during the atmospheric oxidation of VOCs mixtures.

Declaration of competing interest

The authors declare that they have no known competing financial interests or personal relationships that could have appeared to influence the work reported in this paper.

CRediT authorship contribution statement

Yingqi Zhao: Validation, Investigation, Formal analysis, Data curation. **Ya Zhao:** Investigation, Formal analysis, Data curation. **Chong Wang:** Investigation, Formal analysis, Data curation. **Yufeng Shao:** Investigation, Formal analysis, Data curation. **Hua Xie:** Software, Methodology. **Jiayue Yang:** Resources, Methodology. **Weiqing Zhang:** Resources, Methodology. **Guorong Wu:** Resources, Methodology. **Gang Li:** Writing – review & editing, Writing – original draft, Supervision, Funding acquisition, Conceptualization. **Ling Jiang:** Writing – review & editing, Writing – original draft, Visualization, Validation, Supervision, Project administration, Funding acquisition, Conceptualization. **Xueming Yang:** Resources, Project administration, Conceptualization.

Acknowledgments

The authors gratefully acknowledge the staff members of the Dalian Coherent Light Source (No. 31127.02.DCLS) for technical support and assistance in data collection. This work was supported by the National Natural Science Foundation of China (Nos. 22125303, 92361302, 92061203, 22103082, 22273101, 22288201, and 21327901), the Strategic Priority Research Program of the Chinese Academy of Sciences (No. XDB0970100), the National Key Research and Development Program of China (No. 2021YFA1400501), the Innovation Program for Quantum Science and Technology (No. 2021ZD0303304), Dalian Institute of Chemical Physics (No. DICP I202437), Chinese Academy of Sciences (No. GJJSTD20220001), and the International Partnership Program of CAS (No. 121421KYSB20170012).

Appendix A Supplementary data

Supplementary material associated with this article can be found in the online version at doi:10.1016/j.jes.2025.04.020.

References

Ahlberg, E., Falk, J., Eriksson, A., Holst, T., Brune, W.H., Kristensson, A., et al., 2017. Secondary organic aerosol from VOC mixtures in an oxidation flow reactor. Atmos. Environ. 161, 210–220.

Almeida, C., Oliveira-Júnior, J., Delgado, R., Cubo, P., Ramos, M., 2017. Spatiotemporal rainfall and temperature trends throughout the Brazilian Legal Amazon, 1973–2013. Int. J. Climatol. 37, 2013–2026.

Atkinson, R., 2000. Atmospheric chemistry of VOCs and NO_x. Atmos. Environ. 34, 2063–2101.

Atkinson, R., Arey, J., 2003. Atmospheric degradation of volatile organic compounds. Chem. Rev. 103, 4605–4638.

Berkemeier, T., Takeuchi, M., Eris, G., Ng, N.L., 2020. Kinetic modeling of formation and evaporation of secondary organic aerosol from NO_3 oxidation of pure and mixed monoterpenes. Atmos. Chem. Phys. 20, 15513–15535.

Berndt, T., Mentler, B., Scholz, W., Fischer, L., Herrmann, H., Kulmala, M., et al., 2018a. Accretion product formation from ozonolysis and OH radical reaction of α-pinene: mechanistic insight and the influence of isoprene and ethylene. Environ. Sci. Technol. 52, 11069–11077.

Berndt, T., Scholz, W., Mentler, B., Fischer, L., Herrmann, H., Kulmala, M., et al., 2018b. Accretion product formation from self- and cross-reactions of RO_2 radicals in the atmosphere. Angew. Chem. Int. Ed. 57, 3820–3824.
Bian, Q., May, A.A., Kreidenweis, S.M., Pierce, J.R., 2015. Investigation of particle and vapor wall-loss effects on controlled wood-smoke smog-chamber experiments. Atmos. Chem. Phys. 15, 11027–11045.
Boyd, C.M., Nah, T., Xu, L., Berkemeier, T., Ng, N.L., 2017. Secondary organic aerosol (SOA) from nitrate radical oxidation of monoterpenes: effects of temperature, dilution, and humidity on aerosol formation, mixing, and evaporation. Environ. Sci. Technol. 51, 7831–7841.
Burnett, R., Chen, H., Szyszkowicz, M., Fann, N., Hubbell, B., Pope III, C.A., et al., 2018. Global estimates of mortality associated with long-term exposure to outdoor fine particulate matter. Proc. Natl. Acad. Sci. U.S.A. 115, 9592–9597.
Chen, T., Zhang, P., Chu, B., Ma, Q., Ge, Y., Liu, J., et al., 2022. Secondary organic aerosol formation from mixed volatile organic compounds: Effect of RO_2 chemistry and precursor concentration. NPJ Clim. Atmos. Sci. 5, 95.
Dada, L., Stolzenburg, D., Simon, M., Fischer, L., Heinritzi, M., Wang, M., et al., 2023. Role of sesquiterpenes in biogenic new particle formation. Sci. Adv. 9, eadi5297.
Daellenbach, K.R., Uzu, G., Jiang, J., Cassagnes, L.-E., Leni, Z., Vlachou, A., et al., 2020. Sources of particulate-matter air pollution and its oxidative potential in Europe. Nature 587, 414–419.
Draper, D., Farmer, D., Desyaterik, Y., Fry, J., 2015. A qualitative comparison of secondary organic aerosol yields and composition from ozonolysis of monoterpenes at varying concentrations of NO_2. Atmos. Chem. Phys. 15, 12267–12281.
Ehn, M., Thornton, J.A., Kleist, E., Sipilä, M., Junninen, H., Pullinen, I., et al., 2014. A large source of low-volatility secondary organic aerosol. Nature 506, 476–479.
Frisch, M., Trucks, G., Schlegel, H., Scuseria, G., Robb, M., Cheeseman, J., et al., 2016. In: Gaussian 16 Revision C. 01, 2016, 1. Gaussian Inc., Wallingford, CT, p. 572.
Fu, R., Yin, L., Li, W., Arias, P.A., Dickinson, R.E., Huang, L., et al., 2013. Increased dry-season length over southern Amazonia in recent decades and its implication for future climate projection. Proc. Natl. Acad. Sci. U.S.A. 110, 18110–18115.
Griffin, R.J., Cocker III, D.R., Seinfeld, J.H., Dabdub, D., 1999. Estimate of global atmospheric organic aerosol from oxidation of biogenic hydrocarbons. Geophys. Res. Lett. 26, 2721–2724.
Guenther, A., Jiang, X., Heald, C.L., Sakulyanontvittaya, T., Duhl, T.A., Emmons, L., et al., 2012. The model of emissions of gases and aerosols from Nature version 2.1 (MEGAN2.1): An extended and updated framework for modeling biogenic emissions. Geosci. Model Dev. 5, 1471–1492.
Guenther, A., Hewitt, C.N., Erickson, D., Fall, R., Geron, C., Graedel, T., et al., 1995. A global model of natural volatile organic compound emissions. J. Geophys. Res. Atmos. 100, 8873–8892.
Hallquist, M., Wenger, J.C., Baltensperger, U., Rudich, Y., Simpson, D., Claeys, M., et al., 2009. The formation, properties and impact of secondary organic aerosol: current and emerging issues. Atmos. Chem. Phys. 9, 5155–5236.
Hanson, D.R., Sawyer, A., Long, D., Sofio, D., Kunz, J., Wentzel, M., 2022. Particle formation from photooxidation of α-pinene, limonene, and myrcene. J. Phys. Chem. A 126, 910–923.
Iyer, S., Rissanen, M.P., Valiev, R., Barua, S., Krechmer, J.E., Thornton, J., et al., 2021. Molecular mechanism for rapid autoxidation in α-pinene ozonolysis. Nat. Commun. 12, 878.
Jang, M., Czoschke, N.M., Northcross, A.L., 2004. Atmospheric organic aerosol production by heterogeneous acid-catalyzed reactions. Chem. Phys. Chem. 5, 1646–1661.
Jia, L., Xu, Y., 2020. The role of functional groups in the understanding of secondary organic aerosol formation mechanism from alpha-pinene. Sci. Total Environ. 738, 139831.
Jimenez, J.L., Canagaratna, M., Donahue, N., Prevot, A., Zhang, Q., Kroll, J.H., et al., 2009. Evolution of organic aerosols in the atmosphere. Science 326, 1525–1529.
Jokinen, T., Berndt, T., Makkonen, R., Kerminen, V.-M., Junninen, H., Paasonen, P., et al., 2015. Production of extremely low volatile organic compounds from biogenic emissions: Measured yields and atmospheric implications. Proc. Natl. Acad. Sci. U.S.A. 112, 7123–7128.
Jonsson, Å.M., Hallquist, M., Ljungström, E., 2006. Impact of humidity on the ozone initiated oxidation of limonene, Δ^3-carene, and α-pinene. Environ. Sci. Technol. 40, 188–194.
Jonsson, Å.M., Hallquist, M., Saathoff, H., 2007. Volatility of secondary organic aerosols from the ozone initiated oxidation of α-pinene and limonene. J. Aerosol Sci. 38, 843–852.
Kelly, J.M., Doherty, R.M., O'Connor, F.M., Mann, G.W., 2018. The impact of biogenic, anthropogenic, and biomass burning volatile organic compound emissions on regional and seasonal variations in secondary organic aerosol. Atmos. Chem. Phys. 18, 7393–7422.
Kenseth, C.M., Hafeman, N.J., Rezgui, S.P., Chen, J., Huang, Y., Dalleska, N.F., et al., 2023. Particle-phase accretion forms dimer esters in pinene secondary organic aerosol. Science 382, 787–792.
Kiendler-Scharr, A., Wildt, J., Maso, M.D., Hohaus, T., Kleist, E., Mentel, T.F., et al., 2009. New particle formation in forests inhibited by isoprene emissions. Nature 461, 381–384.
Kim, H., Paulson, S.E., 2013. Real refractive indices and volatility of secondary organic aerosol generated from photooxidation and ozonolysis of limonene, α-pinene and toluene. Atmos. Chem. Phys. 13, 7711–7723.
Kirkby, J., Duplissy, J., Sengupta, K., Frege, C., Gordon, H., Williamson, C., et al., 2016. Ion-induced nucleation of pure biogenic particles. Nature 533, 521–526.
Lelieveld, J., Evans, J.S., Fnais, M., Giannadaki, D., Pozzer, A., 2015. The contribution of outdoor air pollution sources to premature mortality on a global scale. Nature 525, 367–371.
Li, J., Li, H., Li, K., Chen, Y., Zhang, H., Zhang, X., et al., 2021. Enhanced secondary organic aerosol formation from the photo-oxidation of mixed anthropogenic volatile organic compounds. Atmos. Chem. Phys. 21, 7773–7789.
Li, Q., Hu, D., Leungsakul, S., Kamens, R.M., 2007. Large outdoor chamber experiments and computer simulations: (I) Secondary organic aerosol formation from the oxidation of a mixture of d-limonene and α-pinene. Atmos. Environ. 41, 9341–9352.
Liu, D., Zhang, Y., Zhong, S., Chen, S., Xie, Q., Zhang, D., et al., 2023. Large differences of highly oxygenated organic molecules (HOMs) and low-volatile species in secondary organic aerosols (SOAs) formed from ozonolysis of β-pinene and limonene. Atmos. Chem. Phys. 23, 8383–8402.
Liu, S., Galeazzo, T., Valorso, R., Shiraiwa, M., Faiola, C.L., Nizkorodov, S.A., 2024. Secondary organic aerosol from OH-initiated oxidation of mixtures of d-limonene and β-myrcene. Environ. Sci. Technol. 58, 13391–13401.
Luo, H., Chen, J., Li, G., An, T., 2021. Formation kinetics and mechanisms of ozone and secondary organic aerosols from photochemical oxidation of different aromatic hydrocarbons: dependence on NO_x and organic substituents. Atmos. Chem. Phys. 21, 7567–7578.
Luo, H., Vereecken, L., Shen, H., Kang, S., Pullinen, I., Hallquist, M., et al., 2023. Formation of highly oxygenated organic molecules from the oxidation of limonene by OH radical: significant contribution of H-abstraction pathway. Atmos. Chem. Phys. 23, 7297–7319.
McFiggans, G., Mentel, T.F., Wildt, J., Pullinen, I., Kang, S., Kleist, E., et al., 2019. Secondary organic aerosol reduced by mixture of atmospheric vapours. Nature 565, 587–593.
Mohr, C., Lopez-Hilfiker, F.D., Yli-Juuti, T., Heitto, A., Lutz, A., Hallquist, M., et al., 2017. Ambient observations of dimers from terpene oxidation in the gas phase: Implications for new particle formation and growth. Geophys. Res. Lett. 44, 2958–2966.
Mutzel, A., Zhang, Y., Böge, O., Rodigast, M., Kolodziejczyk, A., Wang, X., et al., 2021. Importance of secondary organic aerosol formation of α-pinene, limonene, and m-cresol comparing day-and nighttime radical chemistry. Atmos. Chem. Phys. 21, 8479–8498.
Park, J.-H., Babar, Z.B., Baek, S.J., Kim, H.S., Lim, H.-J., 2017. Effects of NO_x on the molecular composition of secondary organic aerosol formed by the ozonolysis and photooxidation of α-pinene. Atmos. Environ. 166, 263–275.
Pathak, R.K., Stanier, C.O., Donahue, N.M., Pandis, S.N., 2007. Ozonolysis of α-pinene at atmospherically relevant concentrations: Temperature dependence of aerosol mass fractions (yields). J. Geophys. Res. Atmos. 112, D03201.
Perakyla, O., Berndt, T., Franzon, L., Hasan, G., Meder, M., Valiev, R.R., et al., 2023. Large gas-phase source of esters and other accretion products in the atmosphere. J. Am. Chem. Soc. 145, 7780–7790.
Piletic, I.R., Kleindienst, T.E., 2022. Rates and yields of unimolecular reactions producing highly oxidized peroxy radicals in the OH-induced autoxidation of α-pinene, β-pinene, and limonene. J. Phys. Chem. A 126, 88–100.
Rolletter, M., Kaminski, M., Acir, I.-H., Bohn, B., Dorn, H.-P., Li, X., et al., 2019. Investigation of the α-pinene photooxidation by OH in the atmospheric simulation chamber SAPHIR. Atmos. Chem. Phys. 19, 11635–11649.
Saathoff, H., Naumann, K.-H., Möhler, O., Jonsson, Å.M., Hallquist, M., Kiendler-Scharr, A., et al., 2009. Temperature dependence of yields of secondary organic aerosols from the ozonolysis of α-pinene and limonene. Atmos. Chem. Phys. 9, 1551–1577.
Seinfeld, J.H., Bretherton, C., Carslaw, K.S., Coe, H., DeMott, P.J., Dunlea, E.J., et al., 2016. Improving our fundamental understanding of the role of aerosol−cloud interactions in the climate system. Proc. Natl. Acad. Sci. U.S.A. 113, 5781–5790.
Shrivastava, M., Cappa, C.D., Fan, J., Goldstein, A.H., Guenther, A.B., Jimenez, J.L., et al., 2017. Recent advances in understanding secondary organic aerosol: Implications for global climate forcing. Rev. Geophys. 55, 509–559.
Spittler, M., Barnes, I., Bejan, I., Brockmann, K., Benter, T., Wirtz, K., 2006. Reactions of NO_3 radicals with limonene and α-pinene: Product and SOA formation. Atmos. Environ. 40, 116–127.
Takeuchi, M., Berkemeier, T., Eris, G., Ng, N.L., 2022. Non-linear effects of secondary organic aerosol formation and properties in multi-precursor systems. Nat. Commun. 13, 7883.
Thomsen, D., Elm, J., Rosati, B., Skønager, J.T., Bilde, M., Glasius, M., 2021. Large discrepancy in the formation of secondary organic aerosols from structurally similar monoterpenes. ACS Earth Space Chem. 5, 632–644.
Thomsen, D., Thomsen, L.D., Iversen, E.M., Björgvinsdóttir, T.đ.N.t., Vinther, S.F., Skønager, J.T., et al., 2022. Ozonolysis of α-pinene and Δ^3-carene mixtures: formation of dimers with two precursors. Environ. Sci. Technol. 56, 16643–16651.
Voliotis, A., Wang, Y., Shao, Y., Du, M., Bannan, T.J., Percival, C.J., et al., 2021. Exploring the composition and volatility of secondary organic aerosols in mixed anthropogenic and biogenic precursor systems. Atmos. Chem. Phys. 21, 14251–14273.
Voliotis, A., Du, M., Wang, Y., Shao, Y., Alfarra, M.R., Bannan, T.J., et al., 2022. Chamber investigation of the formation and transformation of secondary organic aerosol in mixtures of biogenic and anthropogenic volatile organic compounds. Atmos. Chem. Phys. 22, 14147–14175.
Watne, Å.K., Westerlund, J., Hallquist, Å.M., Brune, W.H., Hallquist, M., 2017. Ozone and OH-induced oxidation of monoterpenes: Changes in the thermal properties of secondary organic aerosol (SOA). J. Aerosol. Sci. 114, 31–41.
Wildt, J., Mentel, T., Kiendler-Scharr, A., Hoffmann, T., Andres, S., Ehn, M., et al., 2014. Suppression of new particle formation from monoterpene oxidation by NO_x. Atmos. Chem. Phys. 14, 2789–2804.
Yang, Z., Li, K., Tsona, N.T., Luo, X., Du, L., 2023. SO_2 enhances aerosol formation from anthropogenic volatile organic compound ozonolysis by producing sulfur-containing compounds. Atmos. Chem. Phys. 23, 417–430.
Yao, M., Li, Z., Li, C., Xiao, H., Wang, S., Chan, A.W., et al., 2022. Isomer-resolved reactivity of organic peroxides in monoterpene-derived secondary organic aerosol. Environ. Sci. Technol. 56, 4882–4893.

Ye, J., Abbatt, J.P., Chan, A.W., 2018. Novel pathway of SO_2 oxidation in the atmosphere: reactions with monoterpene ozonolysis intermediates and secondary organic aerosol. Atmos. Chem. Phys. 18, 5549–5565.

Ylisirnioe, A., Buchholz, A., Mohr, C., Li, Z., Barreira, L., Lambe, A., et al., 2020. Composition and volatility of secondary organic aerosol (SOA) formed from oxidation of real tree emissions compared to simplified volatile organic compound (VOC) systems. Atmos. Chem. Phys. 20, 5629–5644.

Zang, X., Zhang, Z., Jiang, S., Zhao, Y., Wang, T., Wang, C., et al., 2022. Aerosol mass spectrometry of neutral species based on a tunable vacuum ultraviolet free electron laser. Phys. Chem. Chem. Phys. 24, 16484–16492.

Zhang, P., Ma, P., Shu, J., Huang, J., Yang, B., Zhang, H., 2019. Characterization of crucial fragments during the nucleation and growth of secondary organic aerosol from the high-NO photo-oxidation of α-pinene. Atmos. Environ. 213, 47–54.

Zhang, S., Du, L., Yang, Z., Tchinda, N.T., Li, J., Li, K., 2023. Contrasting impacts of humidity on the ozonolysis of monoterpenes: insights into the multi-generation chemical mechanism. Atmos. Chem. Phys. 23, 10809–10822.

Zhang, Z., Zhao, Y., Zhao, Y., Zang, X., Xie, H., Yang, J., et al., 2024. Effects of NO and SO_2 on the secondary organic aerosol formation from isoprene photooxidation. Atmos. Environ. 318, 120248.

Zhang, Z., Zhao, Y., Zhao, Y., Zang, X., Xie, H., Yang, J., et al., 2025. Effects of isoprene on the ozonolysis of Δ^3-carene and β-caryophyllene: Mechanisms of secondary organic aerosol formation and cross-dimerization. J. Environ. Sci. 150, 556–570.

Zhao, D., Kaminski, M., Schlag, P., Fuchs, H., Acir, I.-H., Bohn, B., et al., 2015. Secondary organic aerosol formation from hydroxyl radical oxidation and ozonolysis of monoterpenes. Atmos. Chem. Phys. 15, 991–1012.

Zhao, D., Schmitt, S.H., Wang, M., Acir, I.-H., Tillmann, R., Tan, Z., et al., 2018. Effects of NO_x and SO_2 on the secondary organic aerosol formation from photooxidation of α-pinene and limonene. Atmos. Chem. Phys. 18, 1611–1628.

Zhao, Y., Zhang, Z., Zhao, Y., Wang, C., Xie, H., Yang, J., et al., 2024. Effects of NO_x and NH_3 on the secondary organic aerosol formation from α-pinene photooxidation. Atmos. Environ. 337, 120778.

Zhu, W., Guo, S., Shi, J., Song, K., Yu, Y., Tan, R., et al., 2024. Novel findings on molecular SOA fingerprint lists: implications for interaction of multiprecursor oxidation. Environ. Sci. Technol. Lett. 11, 1068–1074.